NEW APPROACH FOR THE CONSTRUCTION OF MESO-SCALE FINITE ELEMENT MODELS OF TEXTILE COMPOSITES WITH PERIODIC BOUNDARY CONDITIONS

S. Jacques[a]*, I. De Baere[a], W. Van Paepegem[a]

[a]*Ghent University, Dept. of Materials Science and Engineering, Technologiepark-Zwijnaarde 903, 9052 Zwijnaarde, Belgium*
**Stefan.Jacques@UGent.be*

Keywords: Textile composites; Mechanical properties; Multiscale modelling; Periodic Boundary Conditions

Abstract
Since experimental testing is labour intensive and time consuming, numerical analysis using Representative Unit Cell (RUC) and Finite Element (FE) analyses for obtaining the elastic material constants have proven to be suitable. One of the drawbacks of the existing techniques is that one is obliged to have identical meshes on opposite faces for applying periodic boundary conditions (PBC), or that multiple part finite element meshes are not allowed. The new ORAS software discussed in this paper allows non-identical meshes at opposite faces and multiple part meshes. The results of the meso-scale FE analysis of the RUC using PBC with macro homogenization obtained with the new technique are in good agreement with those obtained using conventional techniques and experimental data.

1 Introduction

The mechanical behaviour of textile fabric composites is complex because it is a multi-scale problem. The macroscopic behaviour is very dependent on the interactions of the yarns and the matrix at meso-scale (scale of the textile unit cell). Similarly, the behaviour of the unit cell at meso-scale is dependent on the interactions of fibres and fibres and matrix at the interface at micro-scale level. Over the years numerous approaches were developed in order to predict the mechanical behaviour of textile reinforced composites. Depending on the complexity of the architecture of the reinforcement, more or less complicated methods were introduced starting from simple analytical equivalent laminate models to complex "cells" based models representing the 3D geometry of the textile architecture [1,2,3]. Another approach with approximate representation of the reinforcing geometry for obtaining the homogenized elastic properties of the composite RUC uses the averaged properties of differently oriented yarns in the architecture based on the transformation of the stiffness tensor with the reference coordinate system, with the inclusion-based model as a generalisation of this approach [1,3,4]. In order to capture the complex stress-strain fields throughout the RUC, many researches explored the possibility of using the FE calculations. Work from Kabelka (1984), Woo and Whitcomb (1992), Sankar and Marrey (1997) presented solutions for 2D analyses of plain weave composites using the assumption of plain-strain state, but these models are not suitable for correctly modelling textile composites [3]. Yoshino and Ohtsuka (1982), Whitcomb

(1989), Dasgupta et al. (1994), Naik and Ganesh (1992), Paumelle et al. (1991), Blacketter et al. (1993) [5], Glaesgen et al. (1996), MCilhagger and Hill et al. (1995), Lomov et al. (2005), Verpoest and Lomov (2005) and Kurashiki et al. (2005) developed 3D models in combination with homogenization theories viz. kinematic and periodic boundary conditions for the prediction of the macro homogenized elastic properties of textile reinforced RUC. One of the big issues when using any of the 3D models of the reinforcement is correctly defining and modelling the reinforcement architecture since all models use mathematically simplified representations of the cross sections of the yarns (circular, elliptical, lenticular or polygonal) [3]. This leads typically to an underestimation of the fibre volume fractions. Another reason is that for existing PBC techniques either identical meshes at opposite faces are needed with a single part mesh [1,6], either non-identical meshes at opposite faces can be handled but a unique part mesh is needed or unique material is needed. This uniqueness of the parts mesh or material is the drawback of the methods defined in [7,8]. Therefore this paper will present a method allowing the FE meso-scale calculation using PBC with non-identical meshes at opposite faces and allowing multiple parts meshes and multiple materials. The new technique is benchmarked with state of the art techniques and experimental results [9] on a 5 harness satin weave composite.

Advantages of this new approach are: i) no restrictions for yarn shapes (cross section/ undulation) and matrix (voids); ii) use a micro-CT scan as input for CAD generation; iii) all different meshes (tetrahedral, hexahedral) can be handled using FE software; iv) interface layers (cohesive elements) can be implemented easily for the modelling of damage in between the yarns/matrix, yarns/yarns or in the matrix itself.

All functionalities have been grouped in the in-house developed ORAS software (Object oriented, RVE, Assembly, Software).

2 Unit cell modelling

2.1 Material properties

For this research work, the example material used is a thermoplastic 5-harness satin weave composite (CETEX®) with T300JB carbon fibre as reinforcement and PPS (PolyPhenylene Sulfide) as matrix. The fabric geometrical parameters needed for the construction of the RUC geometry such as yarn spacing, yarn width and thickness of the yarns were extracted from a micro-CT analysis [9], together with the parameters of the constituents (carbon fibre and PPS matrix). The material properties of the constituents of the textile composite, the T300JB carbon fibre (E_{11} = 231 GPa; E_{22} = 28 GPa; G_{12} = 24 GPa; G_{23} = 10.7 GPa; ν_{12} = 0.26; ν_{23} = 0.3) and the PPS resin (E = 3.8 GPa; G = 1.38 GPa; ν = 0.37), are used to calculate the impregnated carbon-PPS unidirectional composite material properties (E11 = 162.60 GPa; E22 = 13.70 GPa; G12 = 6.50 GPa; G23 = 5.07 GPa; ν12 = 0.29; ν23 = 0.35) using the analytical Chamis micro-mechanical homogenization formulas [10] with an intra-yarn fibre volume fraction Kf = 0.7.

2.2 Geometrical model

Specialized geometric model pre-processors for building models of the internal structure of textile reinforcements can be found nowadays, with the most well-known being WiseTex and TexGen [11,12]. For many research purposes, one is interested in the impact of the deviation of the geometry compared to the ideal models used in these software packages [13]. The creation of the geometry using commercial CAD software allows having the freedom of creating any yarn shape in longitudinal and transverse directions. Two models (‘Model A’ with yarn height = 0.155 mm and ‘Model B’ with yarn height = 0.156 mm) of the RUC are made in Catia V5 using the parameters of yarns and matrix as given in section 2.1 (Figure 1),

staying within the limits defined by the contours found with the CT scan. The choice of these values was made in order to be able to compare the method developed in this paper to the state of the art technique, according to the fibre volume fractions after meshing. Additionally the difference between the yarn heights of 'Model A' and 'Model B' was implemented in order to study the influence of a small increase of the thickness of the yarns on the global material behaviour.

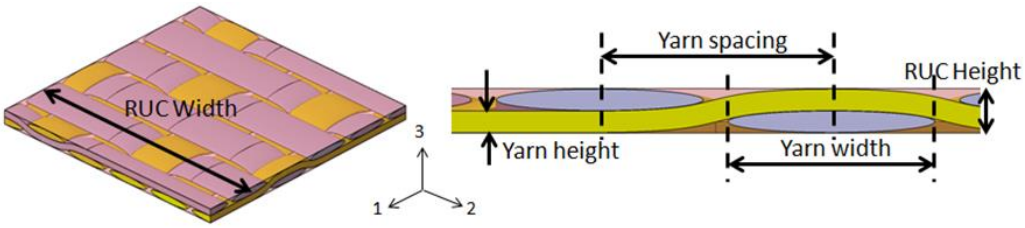

Figure 1: Geometric model of the 5H-satin weave RUC created with a CAD software

2.3 Mesh

The geometrical models are meshed with the pre-processor of commercial FE software (Abaqus™). The yarns were meshed using an advancing front sweep mesh. A 3D 8-node linear structural solid element is used. The matrix has been meshed with 3D 4-node linear tetrahedral elements in order to catch the curvatures of the model. Four mesh models are built 'A-M1', ' B-M2', 'B-M3' and 'B-M4' out of the geometrical models 'Model A' and 'Model B', with the mesh sizes for 'A-M1' and ' B-M2' (Figure 2) similar to the benchmarked model mesh obtained using the MeshTex software [14,15,9]. Since mesh convergence could have an impact on the fibre volume fraction, on the FE results and thus on the homogenized elastic properties for the macro scale composite, model 'B-M3' with the same mesh for the matrix, but with an increased number of elements for the yarn's mesh is created in order to capture the influence of the mesh size of the yarns. Finally in the mesh model 'B-M4' the same yarn mesh as for model 'B-M3' is used with a refined matrix mesh (Figure 2).

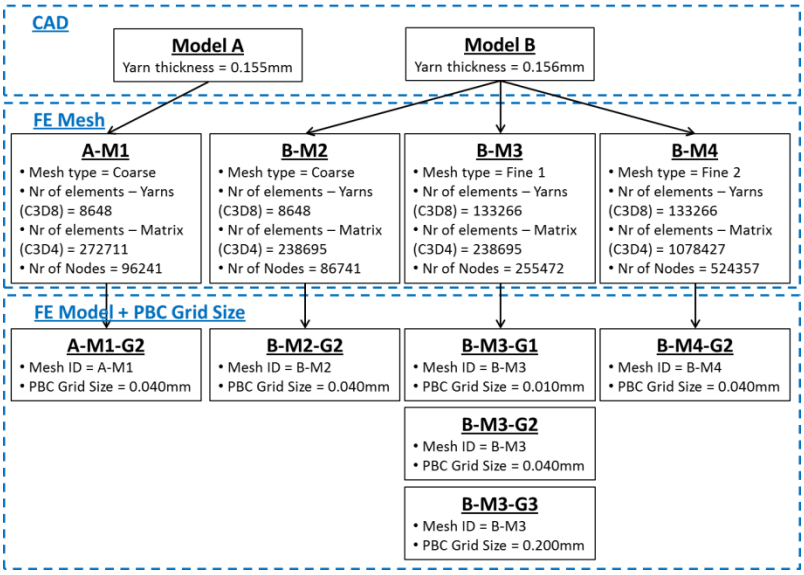

Figure 2: Schematic tree explaining the nomenclature of the different models used, going from the CAD model to the FE mesh model to the calculated FE model + PBC Grid size

The material properties were applied with respect of the local orthotropic orientations within the yarns by using an in-house built software.

2.4 Boundary conditions

2.4.1 Periodic Boundary Conditions

The basic idea of using periodic boundary conditions is to assume that a part on macro level consists of a number of repeated RUC's in which each basic mechanical element, the RUC, determines the global constitutive law of the material on macro level [1,16,17]. This implies that continuity of the displacements at neighbouring faces of the RUC's must be fulfilled and thus any displacement on one side of the RUC must be the same on the opposite side plus or minus some constant [1,17,18]. Not taking into account the rigid displacements and rotations of the RUC, the displacement field for a periodic structure is related to the strain field by the expression:

$$u(\bar{x}) = \bar{\bar{\varepsilon}}\bar{x} + \tilde{u}(\bar{x}) \quad (1)$$

where $\bar{\bar{\varepsilon}}$ in the first term represents the macroscopic strain tensor and $\bar{x}$ the position vector of a material point in the RUC. The second term represents a volume periodic term with zero average value with $\tilde{u}$ being the local displacement field in the RUC. A second condition that has to be met is the anti-periodicity of the traction distributions at the opposite boundaries of the RUC (∂V):

$$\bar{t} = \bar{\bar{\sigma}}\bar{n} \quad (2)$$

When substituting the macroscopic displacement gradients of the unit cell [9] into the periodic equations, one obtains the nine periodic conditions using the axis system as given in Figure 1. The state of the art requires exactly identical meshes on opposite faces of the RUC [1,6]. The current approach offers a new solution in order to allow non-identical meshes and multiple part meshes to be used in PBC.

2.4.2 ORAS software for the implementation of PBC with non-identical meshes at opposite faces

When importing a CAD model of such a RUC into commercially available FE software, the model will consist of multiple parts in an assembly. Even if the cross sections of the yarns and thus the matrix at the opposite faces will be identical, the mesh generated of this assembly will automatically generate parts meshes with different amounts of nodes at the opposite faces due to the complexity of the matrix mesh. Often, for very complex models, the matrix will exist of tetrahedral meshes with non-identical amounts of nodes at opposite faces. In this section a solution will be given for allowing such meshes in PBC definitions making use of the following steps:

1. Creation of a grid comprising all mesh nodes of the domain ∂V of the RUC
2. Definition of reference points for each grid section
3. Constraint definitions at the interfaces

2.4.2.1 Creation of a grid δV

Considering the volume V of a mesh, with two opposite boundary domains $\partial\Omega1$ and $\partial\Omega2$ (the respective faces ABCD and A*B*C*D* (Figure 3(a))), a grid can be made using a user defined grid size for the x, respectively the y direction:

$$\Delta X_i = X_i - X_{i-1}; \qquad \Delta Y_j = Y_j - Y_{j-1}; \qquad \text{with } r_i = \frac{\Delta X_{i+1}}{\Delta X_i}\ ;\ r_j = \frac{\Delta Y_{j+1}}{\Delta Y_j}$$
$$\Delta X_{i+1} = X_{i+1} - X_i; \qquad \Delta Y_{j+1} = Y_{j+1} - Y_j;$$

Using a uniform PBC grid size, $r_i = r_j = 1$, all mesh nodes of ∂V can be distributed into n cells. Since the same grid is used for opposite domains $\partial\Omega1$ and $\partial\Omega2$, the corresponding cells at opposite faces will contain associated mesh nodes. The nodes of the corresponding cells at opposite faces will be given PBC with the technique explained in section 2.4.2.2.

In order to investigate the influence of the PBC grid size, three different uniform PBC grid sizes are used in the FE calculations, with $\Delta X_i = \Delta Y_i$, given in Figure 2.

2.4.2.2 Definition of reference points

In current PBC techniques with identical meshes at opposite faces, each node of one face is linked to the corresponding node at the opposite face using a PBC. If the number of nodes in cell *k* of domain *∂Ω1* (Figure 3 (b)) of the new PBC technique differs from the number of nodes in the corresponding cell *k** of domain *∂Ω2*, the associated nodes cannot directly be linked to each other using the PBC constraint due to the overconstraint of the nodes. In the FE software products it is not allowed to have more than one PBC equation definition at one node of the FE mesh. To avoid this problem, cell k containing the mesh nodes p_i with $i = 1,2,3$ will be linked to a reference node *p*. The spatial coordinates of the reference nodes are obtained by the Laplacian average. If the uniform grid size chosen is very small, with a ΔX_i smaller than the smallest distance between 2 nodes of the same face, one could obtain a grid cell *k* in domain *∂Ω1* containing mesh nodes and an empty associated cell *k** of domain *∂Ω2*. From the floating node $p_n(x_1, y_1)$ of cell *k* of ∂Ω1 (node without associated nodes in the associated cell k* of ∂Ω2) (Figure 3 (b)) a circular area Γ with a user chosen radius *R* (with $R > 2\Delta X_i$) is created. The size of *R* has to be large enough compared to the FE mesh element size in order to find nodes inside the circular area Γ. For all nodes $p \in \Gamma$, one calculates the following objective function (Equation (3)) in order to obtain the mesh node $p_y \neq p_n$ the closest to p_n:

$$\mathrm{Min}\left\{D\left(p(x_i, y_j), p_y((x_1, y_1))\right) \text{ with } p \in \Gamma \mid D = \sqrt{(x_1 - x_i)^2 + (y_1 - y_i)^2}\right\} \qquad (3)$$

The larger *R*, the more nodes will be implemented in the search algorithm and equation (3), the higher the computational time for obtaining the closest point p_y. The node p_y is associated with cell j (Figure 3 (b)) and node p_n is implemented in the same cell. A new reference point using the Laplacian average method including p_n in its calculation is obtained. All reference points are linked to the nodes of the corresponding cell and are then linked to the equivalent reference points of the cells of the opposite domain using the PBC equation. The grid size used will have an influence on the results, since the bigger the grid, the more nodes each cell will contain and the higher the leverage on the nodes associated to a reference point. This technique can be implemented for the different parts meshes of an assembly, and moreover with meshes where nodes are not shared at the interfaces (viz. the interface between matrix and yarns) the technique can be applied to each individual part mesh.

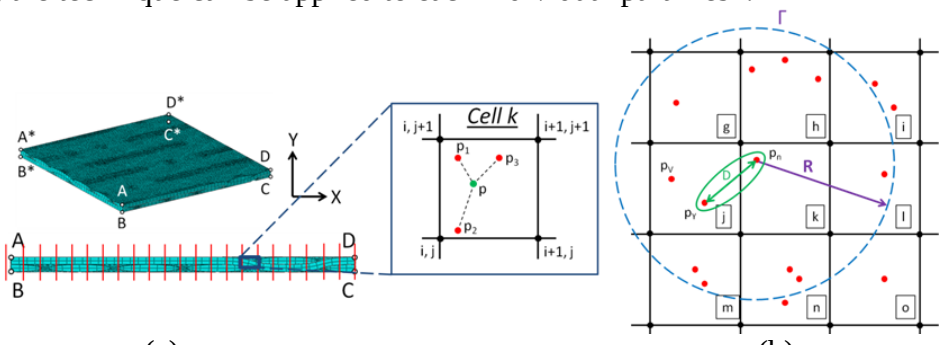

Figure 3: (a) Grid creation of a domain; (b) Redistribution of a floating node

2.4.3 Constraints of the interface surfaces

Since the new technique allows the configuration with multiple parts in an assembly, constraints need to be defined at the interfaces between those parts like: tie constraints, contact definitions, cohesive elements… In the case of a meso-scale FE model, a tie constraint will mostly be chosen as interaction between yarns and matrix parts. This leads to overconstraining the nodes of domain ∂V at the interface between matrix and yarns since a

node at the interface will be implemented in a tie constraint, a Multiple Point Constraint (MPC) constraint and periodic boundary conditions. An error will be generated in the FE software (Abaqus™) since the software will not know which of both constraints has priority, and therefore the displacement of the overconstrained node cannot be calculated. Two methods can be used in order to avoid the overconstraints of the nodes viz. partitioning the parts or erasing the overconstrained nodes in the PBC equations and keeping the tie constraints.

2.5 Homogenization

The relation between homogenized macro strains (ε_{kl}^{H}) and macro stresses (σ_{ij}^{H}) is given by: $\sigma_{ij}^{H} = C_{ijkl}^{H}\varepsilon_{kl}^{H}$ where C_{ijkl}^{H} denotes the elasticity tensor at macro scale. To determine C_{ijkl}^{H} starting from the FE model of the RUC using the periodic boundary conditions, six boundary value models ε_{kl} ($k,l = 1 \dots 3$ and $k \leq l$) have to be solved. Out of the FE results of the six meso-scale models one calculates the homogenized stiffness

$$C_{ijkl}^{H} = \frac{\langle \sigma_{ij} \rangle}{\varepsilon_{kl}} \delta_{ij}\delta_{kl} + \frac{\langle \sigma_{ij} \rangle}{2\varepsilon_{kl}} \delta_{ik}\delta_{jl}\left|\delta_{ij} - 1\right| \quad (4)$$

From this one can calculate the compliance matrix and thus the elastic constants.

3 Validation

3.1 Validation with experimental data

The test, test setup and results of the experiments on the 5-Harness satin weave CF/PPS can be found in [19]. The summary of the obtained results are written in the last column of Table **1**. It should be noted that catching all the anisotropic mechanical properties of a textile composite is a very labour intensive task and almost impossible to determine with the conventional experimental setups.

3.2 Validation of the new technique for the construction of a FE model comprising multiple parts meshes using PBC constraints by comparison with the model obtained with WiseTex/ MeshTex

The difference in yarn thickness of 'model A' and 'model B' described in section 2.3 and the MeshTex model can be explained by the fact that the original yarn thickness of the WiseTex geometrical model is 0.159 mm and is artificially reduced by MeshTex (0.1545 mm) in order to be able to create a mesh for the matrix [9]. In order to be able to validate the new methodology, thicknesses of the yarns were taken for 'model A' and 'model B' which correspond to equivalent V_f as the one obtained using WiseTex/MeshTex ($V_{f,MeshTex}$ = 47.223%; $V_{f,\ A\text{-}M1}$= 47.38%; $V_{f,\ B\text{-}M2}$= 47.687%; $V_{f,\ B\text{-}M3}$= 47.38% and $V_{f,\ B\text{-}M4}$= 48.03%). The slightly higher fibre volume fraction for the new models can be explained by the differences in volumes of the yarns and matrix due to not sharing the nodes at the interface between the matrix and yarns in the models 'A-M1', 'B-M2', 'B-M3' and 'B-M4', whereas there are common nodes at the interface for the 'WiseTex/MeshTex' model.

Models 'A-M1-G2' and model 'B-M2-G2' are compared in order to see the impact of a small difference in the yarn thicknesses on the global macro-scale homogenized elastic constants. The difference in the results for model 'B-M2-G2', model 'B-M3-G2' and model 'B-M4-G2' shows the influence of the mesh size on the results, whereas the difference in results due to the PBC grid size can be noticed by comparing models 'B-M3-G1', 'B-M3-G2' and 'B-M3-G3'. One can notice in Table 1 that the impact will be small for a mesh refinement of the FE model 'B-M2-G2' to model 'B-M3-G2' to model 'B-M4-G2' (Figure 5), but could have an effect on the local strain contours. A good agreement between model 'B-M4-G2', the experimental results and the state of the art WiseTex /MeshTex model can be found (Table **1**). The higher E_{11} of the WiseTex/MeshTex model (+0.3 GPa) in column 3, knowing that the

overall yarn thickness is lower (0.1545 mm) compared to 0.156mm for the CAD model 'B' and thus a lower fibre volume fraction, can be explained as follows:

- The influence due to the decrease of the yarn thickness is not negligible as can be noticed by the increase of the stiffness E_{11} by 0.36 GPa between model 'A-M1-G2' and 'B-M2-G2' with an increase of only 0.001 mm.
- Since the volume of the elements in the cross over points in the WiseTex/MeshTex model is higher than the overall thickness of the yarns, the total volume of these elements in the volume averaging technique will have an impact on the homogenized material property results for the stiffness in the main directions E_{11} and E_{22}.

The mesh convergence between model 'B-M2-G2' and 'B-M4-G2' shows a decrease of the E33 of 0.09 GPa due to the lower interpenetration of the mesh elements of the yarns and matrix. By comparing columns 6, 7 and 8 in Table 1, one notices that the homogenized macro elastic constants can be overestimated if the chosen PBC grid size is too coarse ('B-M3-G3'). This is due to the higher leverage on the nodes in a PBC grid cell, because of the higher distance between the reference node on which the PBC constraint is put and the FE mesh node (Figure 4).

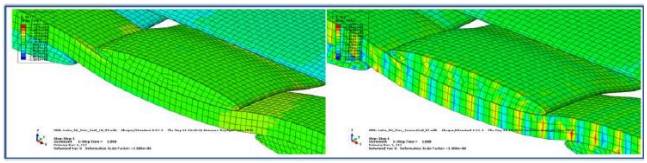

Figure 4: Effect of leverage on the FE results for the RUC due to the grid size choice

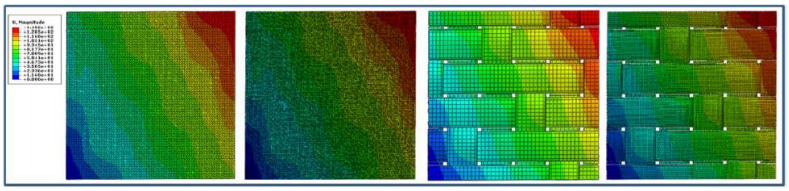

Figure 5: Displacement magnitude results for the FE results of thr RUC with different mesh sizes with PBC

	PBC ORAS	PBC SotA	A-M1-G2	B-M2-G2	B-M3-G1	B-M3-G2	B-M3-G3	B-M4-G2	Experiment
E_{11}, *[GPa]*	56.56	56.50	55.86	56.22	56.24	56.20	57.33	56.20	57±1
E_{22}, *[GPa]*	56.54	56.47	55.84	56.20	56.20	56.20	57.12	56.21	57±1
E_{33}, *[GPa]*	10.55	10.53	10.68	10.75	10.66	10.66	10.63	10.66	-NA-
ν_{12}, *[-]*	0.08	0.08	0.08	0.08	0.08	0.08	0.07	0.08	0.05±0.02
ν_{13}, *[-]*	0.42	0.42	0.42	0.42	0.42	0.42	0.42	0.42	-NA-
ν_{23}, *[-]*	0.42	0.42	0.42	0.42	0.42	0.42	0.42	0.42	-NA-
G_{12}, *[MPa]*	4354.48	4344.91	4382.51	4404.63	4399.86	4398.32	4439.57	4390.28	4360±60
G_{13}, *[MPa]*	3179.14	3160.52	3214.53	3244.98	3231.36	3228.67	3246.34	3227.19	-NA-
G_{23}, *[MPa]*	3180.31	3160.85	3212.70	3245.06	3231.07	3228.96	3239.40	3228.68	-NA-

Table 1: Validation of the FE results of the elastic constants of a 5H-satin Weave CF/PPS composite

4 Conclusions

A method for the construction of meso-scale FE models of textile reinforced composites using periodic boundary conditions on multiple part meshes (ORAS) has been developed and defined. The technique has been validated by comparison to experimental results and to the state of the art validated models (WisTex/MeshTex) for a 5H-satin weave unit cell. This new technique opens new paths for the research of complex meso-scale architectures of textile composites.

5 Acknowledgements

The authors would like to acknowledge TenCate for supplying the composite materials

References

[1] Stepan V Lomov and et al, "Meso-FE modelling of textile composites: Road map, data flow and algorithms," *Composites Science and Technology*, vol. 67, no. 9, pp. 1870-1891, 2007.

[2] Brian N Cox and Gerry Flanagan, *Handbook of Analytical Methods for Textile Composites*. Hampton: National Aeronautics and Space Administration, Langley Research Center, 1997.

[3] Christopher M Pastore, "Opportunities and Challanges for Textile Reinforced Composites," *Mechanics of Composite Materials*, vol. 36, no. 2, pp. 97-116, 2000.

[4] A E Bogdanovich and Christopher M Pastore, *Mechanics of Textile and Laminated Composites*. London: Chapman & Hall, 1996.

[5] D M Blackketter, D E Walrath, and A C Hansen, "Modeling Damage in a Plain Weave Fabric-Reinforced Composite-Material," *Journal of Composite Technology & Research*, vol. 15, no. 2, pp. 136-142, 1993.

[6] Peter Linde, Peter Middendorf, Björn Van Den Broucke, and Henk De Boer, "Numerical Simulation of Damage Behaviour of Textile Reinforced Composites in Aircraft Structures," in *ICAS*, Nice (France), 2010.

[7] Zheng Yuan and Jacob Fish, "Toward realization of computational homogenization in practice," *Int. J. Numer. Meth. Engng*, vol. 73, pp. 361-380, 2008.

[8] V.-D. Ngyuen, E Béchet, C Geuzaine, and L Noels, "Imposing periodic boundary condition on arbitrary meshes by polynomial interpolation," *Computational Materials Science*, vol. 55, pp. 390-406, 2012.

[9] Subbareddy Daggumati, *Concurrent Modelling and Experimental Analysis of Meso-Scale Strain Fields and Damage in Woven Composites under Static and Fatigue Tensile Loading*. Ghent: Ghent University, 2011, PhD Thesis - ISBN 9789085784258, https://biblio.ugent.be/publication/3259370.

[10] C.C. Chamis, "Mechanics of Composite Materials: Past, Present and Future," *NASA Technical Memorandum*, vol. 100793, 1984.

[11] I Verpoest and SV Lomov, "Virtual textile composites software WiseTex: integration with micro-mechanical, permeability and structural analysis.," *Composites Science and Technology*, vol. 65, no. 15-16, pp. 2563-74, 2005.

[12] TexGen. texgen.sourceforge.net. [Online]. http://texgen.sourceforge.net/index.php/Main_Page

[13] Norris F Dow, V Ramnath, and B Walter Rosen, "Analysis of Woven Fabrics for Reinforced Composite Materials," National Aeronautics and Space Administration, Hampton, Technical report 1987.

[14] SV Lomov, X Ding, S Hirosawa, and et al., "FE simulations of textile composites on unit cell level: validation with full-field strain measurements.," in *Proc SAMPE Europe International Conference*, 2005, pp. 28-33.

[15] T Kurashiki, M Zako, S Hirosawa, SV Lomov, and I Verpoest, "Estimation of a mechanical characterization for woven fabric composites by fem based on damage mechanics," in *ECCM-11, 11th European Conference on Composite Materials*, 2004.

[16] V Carvelli and C Poggi, "A homogenization procedure for the numerical analysis of woven fabric composites," *Composites: Part A*, vol. 32, pp. 1425-1432, 2001.

[17] John Whitcomb, Kanthikannan Srirengan, and Clinton Chapman, "Evaluation of homogenization for global/local stress analysis of textile composites," *Composite Structures*, vol. 31, pp. 137-149, 1995.

[18] Jacob Aboudi, Marek-Jerzy Pindera, and Steven M Arnold, "Higher-order theory for periodic multiphase materials with inelastic phases," *International Journal of Plasticity*, vol. 19, pp. 805-847, 2003.

[19] Ives De Baere, Stefan Jacques, Wim Van Paepegem, and Joris Degrieck, "Study of the Mode I and Mode II interlaminar behaviour of a carbon fabric reinforced thermoplastic," *Polymer Testing*, vol. 31, no. 2, pp. 322-332, April 2012.